SOL–GEL SYNTHESIS AND CHARACTERIZATION OF NANOSTRUCTURED HYDROXYAPATITE POWDER

A. Hanifi[1], M. H. Fathi[2]
Materials Science and Engineering Department, Isfahan University of Technology, Esfahan, Iran
Email: a.hanifi@gmail.com

Abstract-**Nanocrystalline powders of hydroxyapatite (HA) were prepared from $Ca(NO_3)_2{\cdot}4H_2O$ and P_2O_5 using a simple sol–gel approach. X-ray diffraction (XRD) indicates the presence of amorphous hydroxyapatite (HA) in the as-dried gel precursor. X-ray patterns collected on the powder after heat-treatment at 600ºC in air exhibits single phase of HA. Scanning electron microscopy (SEM) and Transmission electron microscopy (TEM) show that the powder obtained after heat-treatment at 600ºC is agglomerated and composed of nanocrystalline (30–35 nm) HA particles.**

Keywords **- Hydroxyapatite, Sol-gel- Nanoparticle**

I. INTRODUCTION

Thanks to its chemical and structural similarity with the mineral phase of bone and teeth, synthetic hydroxyapatite, $Ca_{10}(PO_4)_6(OH)_2$ (HA), is widely used for hard tissues repair. The different clinical applications involve repair of bone defects, bone augmentation, as well coatings for metallic implants [1, 2].

For this reason, many HA synthesis techniques have been developed. These include mechanochemical synthesis [3], combustion preparation [4], and various techniques of wet chemistry, such as direct precipitation from aqueous solutions [5], electrochemical deposition [6], sol–gel procedures [7], hydrothermal synthesis [8], and emulsion or micro-emulsion routes [9], etc.

Low-temperature formation and fusion of the apatite crystals has been the main contributions of the sol–gel process, in comparison to conventional methods. For instance, temperatures higher than 1000ºC are usually required to sinter the fine apatite crystals prepared from wet precipitation, whilst several hundred degree Celsius lower than above are needed to densify sol–gel HA [10,11]. Moreover, processing of sol–gel HA usually results in a fine-grain microstructure containing a mixture of nano-to-submicron crystals, better accepted by the host tissue.

The sol–gel product is characterized by nano-size dimension of the primary particles, and this small domain is a very important parameter to improve the contact reaction and the stability at the artificial/natural bone interface. Moreover, the high reactivity of the sol–gel powder allows a reduction of the processing temperature and of any degradation phenomena occurring during sintering. The major limitation to sol–gel technique application is linked to the possible hydrolysis of phosphates and the high cost of the raw materials [12]. Both problems are solved in the method proposed in the present paper where a new process to prepare a pure HA powder via the sol–gel route is present.

II. METHODOLOGY

A designed amount of phosphoric pentoxide (P_2O_5, Merck) was dissolved in absolute ethanol to form a 0.5 mol/l solution. A designed amount of calcium nitrate tetrahydrate ($Ca(NO_3)_2.4H_2O$, Merck) was also dissolved in absolute ethanol to form a 1.67 mol/l solution.

The two solutions were mixed in a Ca/P molar ratio of 1.67 as an initial mixed precursor solution. The mixture was continuously stirred about 24 h at ambient temperature, here a white transparent gel was obtained. The gel was dried at 80ºC for 24 h in an air oven. The dried gels were individually heated at 5 ºC/min^{-1} to 600,700 ºC in a muffle furnace for 0-6 h for each temperature, and then placed in air cooling to ambient temperature.

The sintered products were crushed Powders produced were characterized by X-ray diffraction (XRD). The XRD patterns were recorded using CuKα radiation generated at 40 kV and 100 mA, in the range of 20 º<2θ<80º at a scan speed of 4º/min. Morphological observations of powders were performed in a scanning electron microscopy (SEM) transmission electron microscope (TEM).

III. RESULTS & DISCUSSION

A. XRD analyses

Fig. 1 shows the XRD patterns for a powder sintered at 600ºC. The d spacing are compared with the JCPDS [13] standard for HA in Table 1. It can be seen that there is a good match with the standard both in terms of intensity and position of the lines.

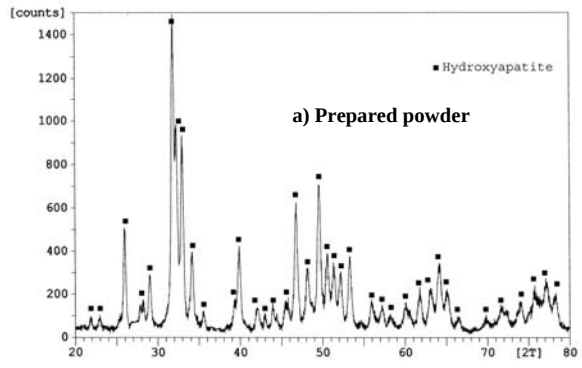

Fig. 1. X-Ray Diffraction pattern of a) Prepared powder and b) Traditional HA powders XRD.

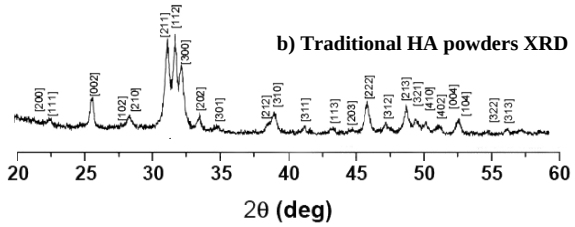

Fig. 1. Continue

TABLE I
d spacing in compare with JCPDC card.

d(nm)		Intensity		hkl
Experimental	JCPDC	Experimental	JCPDC	
0.3446	0.3440	37.0	40	002
0.3085	0.3080	12.4	18	210
0.2814	0.2814	100	100	211
0.2624	0.2631	24.4	25	202
0.2254	0.2262	30	20	310
0.1941	0.1943	27.2	30	222
0.1889	0.1890	22.5	16	312
0.1838	0.1841	28.7	40	213
0.1725	0.1722	24.4	20	004

Fig. 2, 3 demonstrates that the sintering temperature plays an important role in the formation of HA. As the sintering temperature is increased from 600 to 700 ºC, several of the HA lines become more distinct at higher temperatures, and also the widths of the lines become more narrow, which suggests an increase in the crystallite degree. It can also be seen that additional crystalline phases (β-TCP and CaO) appear at 700ºC, and no other crystalline phase presents besides HA at 600 ºC. It could be concluded that HA could be decomposed into β-TCP and CaO as the sintering temperature is at 700ºC or above. The reaction is proposed as follows:

$Ca_{10}(PO_4)_6(OH)_2 = 3Ca_3(PO_4)_2 + CaO + H_2O$

So to obtain the pure HA, the sintering temperature should be below 700 ºC.

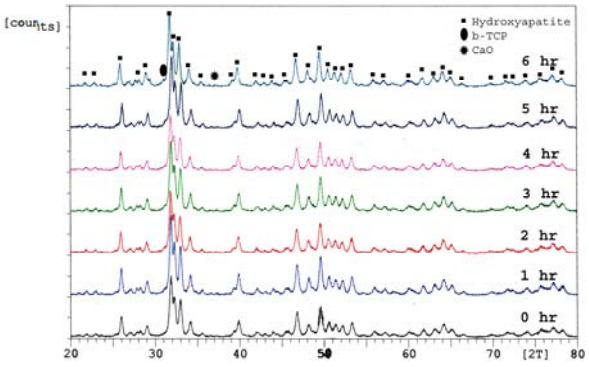

Fig 2. Effect of sintering time on the X-ray patterns of sintered powders in 600ºC

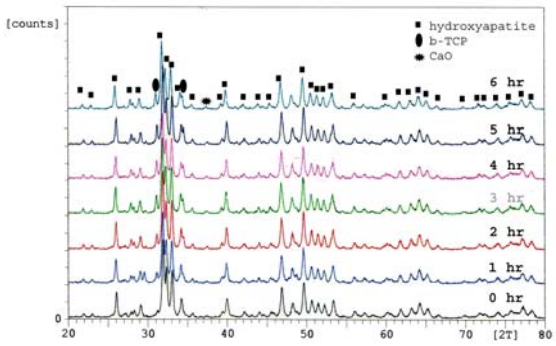

Fig 3. Effect of sintering time on the X-ray patterns of sintered powders in 700ºC

The grain size of products was measured with the Scherrer's equation.

$t = 0.89\lambda / B \cos\theta$

Where t is grain size, λ wavelength of the X-ray tube, B width of peak in the middle of its height and θ Bragg's angle.

Table 2 shows the results of this measuring. As be seen with the increasing of temperature and time of the sintering treatment, the particle size of powders is increased. Because of the extraction of polymeric chains with the firing of amorphous powders that obtained from drying step, there is no obstacle for grain growth. Hence the size of particles is increased and grain growth happened.

TABLE II
Grain size (nm) obtained from Scherrer's equation.

Temperature/Time	0 hr	1 hr	2 hr	3 hr	4 hr	5 hr	6 hr
600 ºC	25	26	27	28	28	28	28
700 ºC	30	31	32	32	32	32	35

B. SEM analyses

Which is presented in Fig. 4 There is no crystalline HAP phase observed in the as-dried state of the gel, indicating that HAP remains amorphous. All the peaks shown in Fig. 5(a) correspond to calcium nitrate implying the incomplete reaction between $Ca(NO_3)_2{\cdot}4H_2O$ and P_2O_5 Crystalline HAP appears to form only after the heat-treatment at 600 ◦C in stagnant air (see Fig. 2), Fig. 5 shows the SEM images of the as-dried gel precursor and the powder obtained after heat-treatment at 600 ◦C. The as-dried gel powders appear to be highly agglomerated caused primarily by the various processes occurring during drying of the gel precursor. It is also possible that the small particles seen embedded in each agglomerated cluster correspond to the calcium nitrate particles, which could be obtained from the recrystallization of the dissolved calcium nitrate during gel formation and the subsequent drying process. The powder obtained after heat-treatment at 600ºC exhibits the morphology of sintered platelets as shown in Fig. 5(b). It appears that very fine particles of HA (30–35 nm) have been sintered slightly during heat-treatment based on the observed fracture surface of the particles seen in the SEM image.

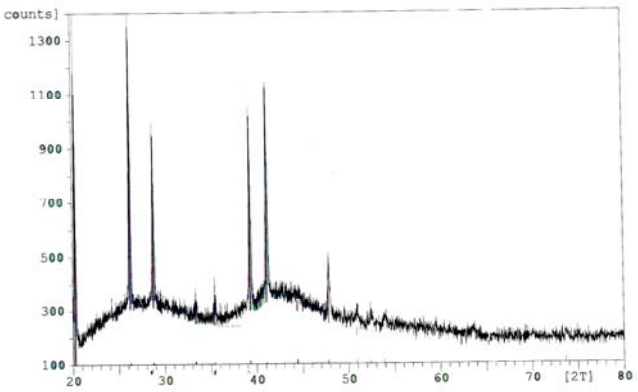

Fig. 4. XRD Pattern of as-dried state of the gel

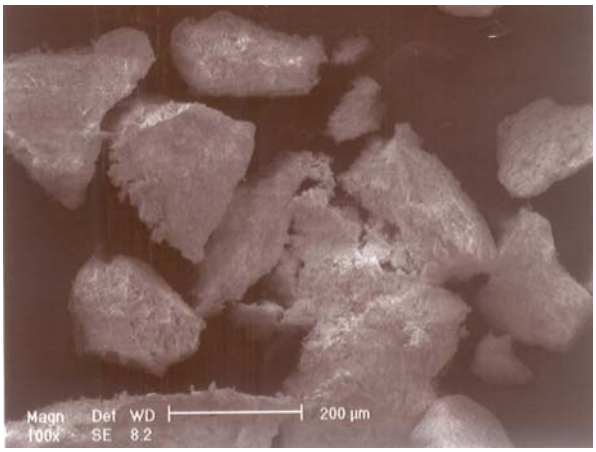

a

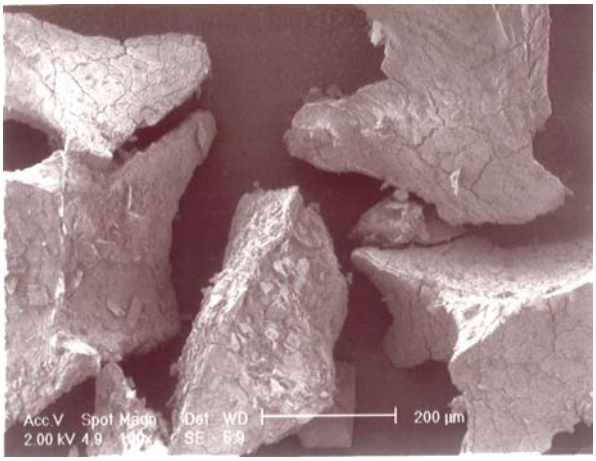

b

Fig. 5. SEM micrograph of a) as-dried gel and b) sintered powder in 600 ºC

C. TEM analyses

Fig. 6 shows the micrograph of the HA powders sintered at 600 and 700 ºC. The HA samples showed nano-sized ellipse-like morphology. However, the powder sintered in 600ºC were only 30 nm size, the powders sintered in 700ºC has the size more than 30 nm. It suggests that the powders

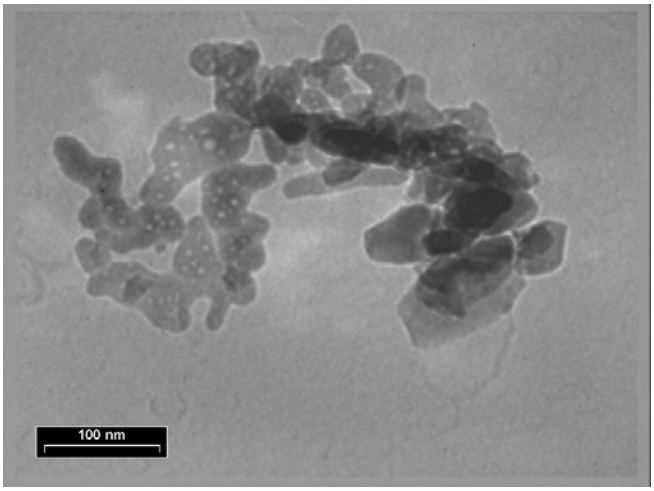

a

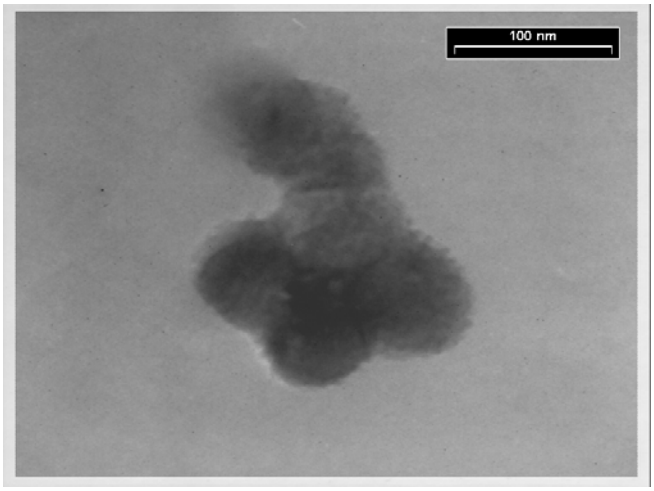

b

Fig .6. TEM micrograph of sintered powders in a) 600 ºC and b) 700 ºC.

synthesized for higher sintering temperature were larger than those for lower sintering temperature, that is, high sintering temperature could contribute to powder growth and agglomerate.

The first stage after making the sol is gelation, where sufficient polymerization has occurred to form a cross linking of the molecules making up the skeletal structure. The next stage is aging. The third stage is drying, during which excess solvent is removed. The final stage is sintering, during which the porous structure is eliminated, the residual organisms are removed, and the minerals are crystallized.

If we use the higher sintering temperatures because of lack of any obstacle for particle growth, the particle size will increase.

IV CONCLUSION

This sol–gel method provides a simple route for synthesis of hydroxyapatite nanopowders. The crystalline degree and morphology of the resulting nanopowders are dependent on the sintering temperature and time. The crystalline degree of

the HA nanopowders increases with the increase of firing temperature, and HA can decompose at 700ºC and above 700ºC. The crystal size of the HA nanopowders increases with the increase of sintering time and temperature. The size of HA nanopowders sintered at 600 is 30 nm.

REFERENCES

[1] L.L. Hench, J. Wilson (Eds.), "An Introduction to Bioceramics", *World Scientific*, Singapore, 1993.

[2] W. Suchanek, M. Yoshimura, J. *Mater. Res*. 13 (1998) 94–117.

[3] W. Kim, Q.W. Zhang, F. Saito, J. *Mater. Sci*. 35 (2000) 5401.

[4] A.C. Tas, J. *Eur. Ceram*. Soc. 20 (2000) 2389.

[5] Lopez-Macipe, R. Rodriguez-Clemente, A. Hidalgo-Lopez, I. Arita, M.V. Garcia-Garduno, E. Rivera, V.M. Castano, J. *Mater. Synth. Process*. 6 (1998) 121.

[6] L.Y. Huang, K.W. Xu, J. Lu, J. *Mater. Sci., Mater. Med*. 11 (2000) 667.

[7] W.J. Weng, J.L. Baptista, *Biomaterials* 19 (1998) 125.

[8] M. Yoshmura, H. Suda, K. Okmoto, K. Loku, J. *Mater. Sci.* 29 (1994) 3399.

[9] G.K. Lim, J. Wang, S.C. Ng, L.M. Gan, J. *Mater. Chem*. 9 (1999) 1635.

[10] Hwang K, Song J, Kang B, Park Y. "Sol–gel derived hydroxyapatite films on alumina substrates", *Surf Coat Tech* 2000; 123:252–5.

[11] Layrolle P, Ito A, Takishi T. "Sol–gel synthesis of amorphous calcium phosphate and sintering into microporous hydroxyapatite bioceramics", J *Am Ceram Soc* 1998;81(6):1421–8.

[12] Jillavenkatesa, R.A. Condrate, J. *Mater. Sci*. 33 (1998) 4111.

[13] JCPDS Card No. 9-432, 1994.